2017 IEEE/RSJ International Conference on Intelligent Robots and Systems (IROS)
September 24–28, 2017, Vancouver, BC, Canada

3D Walking and Skating Motion Generation Using Divergent Component of Motion and Gauss Pseudospectral Method

Noriaki Takasugi, Kunio Kojima, Shunichi Nozawa, Kei Okada and Masayuki Inaba

Abstract— **This paper presents a COM trajectory generation method for 3D walking and skating motion by nonlinear optimization. In our method, we solve the following problems: (1) dealing with both walking and skating motion in the same framework, (2) generating center of mass (COM) trajectory faster than execution time, (3) executing motion with large acceleration. For solving (1) and (2), we calculate the COM trajectory at every step and introduce frictional constraints to the Divergent Component of Motion as terminal conditions. By changing the terminal condition, we can generate both skating and walking motion. Besides, the nonlinear constrained optimization using Gauss Pseudospectral Method is introduced for solving (2) and (3). Thanks to this method, we generate the 3D COM trajectory considering contact constraints and kinematic constraints faster than execution time. Finally, the walking and skating experiment were carried out to confirm the effectiveness of our method using life-sized humanoid HRP-2. Applying the proposed method, HRP-2 could successfully walk at 0.4 [m/s] and skate at 1.0 [m/s].**

I. INTRODUCTION

Locomotion is important and challenging exercise for life-sized humanoid robots. Among locomotion, walking motion is robust and stable on the uneven terrain. Conversely, on the smooth surfaces, the locomotion using wheel such as skating motion is more efficient and faster than walking motion. In our research, we focus on both walking and skating motion (Fig.1) for adaptive locomotion to the environment.

There are many studies about walking motion. The life-sized humanoid robot achieved robust and stable walking motion on the uneven terrain [1], [2]. However, there are few studies about humanoid skating motion. Small-sized humanoid robots achieved skating motion with a roller skate [3] or ice skate [4]. In previous work, we proposed the real-time control method for skating motion and HRP-2 could accelerate and skate on the skateboard at 0.5[m/s] [5]. However, in our previous approach, we could not deal with faster skating motion because we used the linear inverted pendulum model [6] and we didn't optimize trajectory considering kinematics or contact constraints.

In this paper, we propose a motion generation method using nonlinear constrained COM trajectory optimization for humanoid walking and skating motion. We conducted walking and skating motion experiment using life-sized humanoid HRP-2 to show the effectiveness of the proposed method.

N. Takasugi, K. Kojima, S. Nozawa, K. Okada and M. Inaba are with Department of Mechano-Informatics, The University of Tokyo, 7-3-1 Hongo, Bunkyo-ku, Tokyo 113-8656, Japan takasugi at jsk.t.u-tokyo.ac.jp

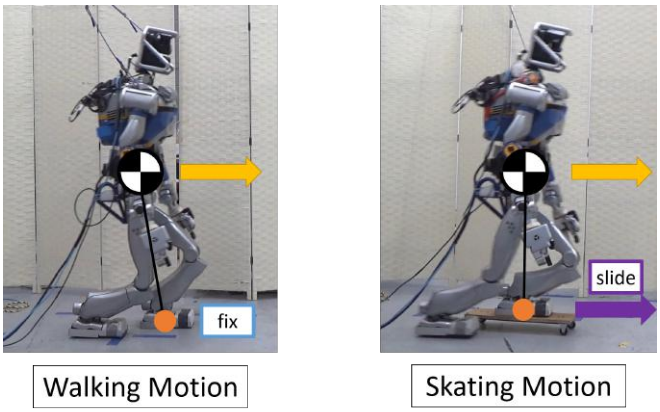

Fig. 1. Walking motion and Skating motion

II. SKATING AND WALKING MOTION OPTIMIZATION AND CONTROL

A. Model and Terms for Walking and Skating Motion

In this research, we deal with two kinds of contact point: static contact and skating contact. Skating motion has both static and skating contact whereas walking motion has only static contact. We introduce linearized coulomb friction cone to describe static, skating and sliding contact as shown in Fig.2. In comparison with the static contact and the sliding contact, the skating contact is static in one direction and dynamic in the other direction. Therefore skating contact has both static friction coefficient and dynamic friction coefficient. In our research, the dynamic friction coefficient of the skating contact is zero.

We define two phases of the skating motion: accelerating phase and sliding phase. In the accelerating phase, the robots push the ground and accelerate them. The robots have both static and skating contact in the accelerating phase. In the sliding phase, the robots slide with one foot whose contact is skating contact. For simplification, we deal with only static contact constraints to generate COM trajectory in the accelerating phase. In addition, we consider single skating contact constraints for the skating motion stability.

B. Related Works

1) Skating Motion or Motion utilizing sliding contact: There are some studies about motions utilizing sliding contact by life-sized humanoid robots. Miura et al. realized the slip turn by HRP-2 and HRP-4 using the simple rotational contact model [7],[8],[9]. Hashimoto et al. proposed the quick turning method by slipping motion which can switch ground contact conditions and demonstrated the slip turn by

978-1-5386-2682-5/17/$31.00 ©2017 IEEE

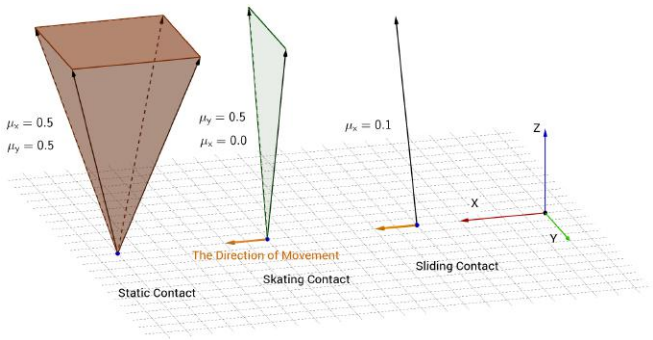

Fig. 2. Friction cones of static and skating contact

WABIAN-2R [10]. However, these studies deal with comparative static motion and it is difficult to apply fast locomotion. Kojima et al. achieved life-sized humanoid slipping motion by controlling foot force [11]. Their method considers dynamics and dynamic friction constraints. However, it is difficult to generate the motion in less time it requires to execute.

There are few studies about skating motion by life-sized humanoid robots. Hashimoto et al. realized skating motion by a biped robot [12]. However, their method cannot consider friction constraints and kinematic constraints. In previous work, we proposed real-time skating motion controller and achieved life-sized humanoid skating motion at 0.5[m/s] [5]. In this paper, we aim to achieve faster skating motion by using nonlinear constrained optimization.

2) Walking Motion Generation and Optimization: First, we refer to the walking motion generation using linear optimal control. Kajita's preview controller based on zero moment point (ZMP) and Linear Inverted Pendulum (LIP) is one of the representative studies [13]. What is more, in the studies [14], Kajita et al. proposed the walk motion controller on a low friction floor considering necessary friction constraints. In [15], Tedrake proposed a time-varying linear-quadratic regulator to track reference ZMP. These methods enable fast computation. Yet these methods assume the height of COM is constant.

Next, in previous studies about three dimensional COM trajectory generation, Takenaka et al. introduced the Divergent Component of Motion (DCM) as unstable part of the COM dynamics and achieved running motion [16]. Moreover, Englsberger et al. proposed the three dimensional walking control by the DCM [1]. In our study, we introduce frictional constraints to DCM for skating motion. Feng et al. proposed online 3D walking optimization using Differential Dynamic Programming (DDP) [2]. Their studies achieved stable and fast walking motion by Atlas. Still, their method cannot deal with frictional constraints and it is difficult to apply skating motion. Dai et al. proposed robust planning method considering frictional constraints and support polygon constraints using the convex optimization and COM admissible region [17]. Caron et al. also introduced ZMP support areas with frictional constraints [18]. Kudruss et al. proposed the nonlinear constrained COM trajectory optimization by direct multiple shooting and applying their method, HRP-2 climbed stairs with the use of a handrail [19]. However, it is difficult to apply their methods to unstable skating motion because their method cannot consider stability in the sliding phase of the skating motion.

In previous studies which apply whole-body motion optimization to the real robot, Lengagne achieved various motions by HRP-2 using B-spline time parameterization [20]. However, there are still problems about a large amount of computation time. On the other hand, Hereid et al. proposed online nonlinear optimal trajectory generation using Hybrid Zero Dynamics (HZD) and Pseudospectral Method [21].Applying this method, Hereid achieved efficient walking motion and online velocity modification by DURUS-2D. In our study, we apply Pseudospectral Method for generating three dimensional COM trajectory for generating trajectory faster than execution time. In addition, we aim to generate not only walking motion but also skating motion.

C. Contribution of This Paper

The contribution of this paper is to propose the way to generate 3D COM trajectory for walking and skating motion considering contact constraints and kinematic constraints faster than execution time. Our method can generate both walking and skating motion by changing the next foot step velocity and friction coefficient. These features enable the robot to execute fast and robust locomotion changing the type of locomotion according to the environment.

III. COM Trajectory Optimization

We describe the nonlinear optimization of the COM trajectory at every step. First, in Subsection. III-A, we provide details of Gauss Pseudospectral Method using for nonlinear optimal control. In Subsection. III-B, we formulate the COM dynamics. Next, we introduce kinematic constraints and contact constraints for acceleration and balancing in Subsection. III-C. Detailed boundary conditions for stable continuous motions is presented in Subsection. III-D Finally, we show the solution of the nonlinear programming problem in Subsection. III-E.

A. Gauss Pseudospectral Method

We use Pseudospectral Method for the nonlinear trajectory optimization. Pseudospectral Method transcribes a continuous optimal control problem into an NLP by discretizing state and control. Among various type of Pseudospectral Methods, we use the Gauss Pseudospectral Method (GPM) [22]. As illustrated in [22], the GPM has high accuracy of the solutions and equivalence between direct and indirect form than other Pseudospectral methods. In the following, we explain details of the GPM.

1) Continuous Optimal Control Problem: We solve the following continuous optimal control problem described using normalized time $\tau \in [-1, 1]$, the state trajectory $\boldsymbol{x}(\tau)$

and the control trajectory $\boldsymbol{u}(\tau)$.

$$\begin{aligned}&\min_{u} J(\boldsymbol{x}(\tau), \boldsymbol{u}(\tau))\\ &\text{where}\\ &\frac{d\boldsymbol{x}}{d\tau} = \frac{t_f - t_0}{2} f\left[\boldsymbol{x}(\tau), \boldsymbol{u}(\tau)\right]\\ &C_c\left[\boldsymbol{x}(\tau), \boldsymbol{u}(\tau)\right] \geq \mathbf{0}\\ &C_b\left[\boldsymbol{x}(-1), \boldsymbol{x}(1)\right] = \mathbf{0}\end{aligned} \tag{1}$$

where J is the cost function, $f\left[\boldsymbol{x}(\tau), \boldsymbol{u}(\tau)\right]$ is the dynamical system. C_c is the function which describes the constraints of the state and control trajectory. C_b is the function which describes the boundary conditions. t_0 is initial time and t_f is the final time. Here, normalized time τ is transformed to $t \in [t_0, t_f]$ in the following equation.

$$t = \frac{t_f - t_0}{2}\tau + \frac{t_f + t_0}{2} \tag{2}$$

2) Discretization of the Trajectory: The GPM is based on the theory of orthogonal collocation and uses the N-Legendre-Gauss (LG) nodes as the collocation points. N-LG nodes are given by the roots of the following Legendre polynomial.

$$P_N(x) = \frac{1}{2^N N!}\frac{d^N}{dx^N}\left[(x^2-1)^N\right] \tag{3}$$

Using the the roots of (3) and -1 and 1, the nodes are defined as $\tau_i \in [-1, 1]$ $(i = 0, 1, 2\cdots N+1)$. By using $N+1$ nodes and $N+1$ Lagrange interpolating polynomials, the state trajectory is approximated as follows.

$$\boldsymbol{x}(\tau) \approx \sum_{i=0}^{N} X(\tau_i) L_i^{N+1}(\tau) \tag{4}$$

$$L_i^{N+1}(\tau) = \prod_{j=0, j\neq i}^{N} \frac{\tau - \tau_j}{\tau_i - \tau_j} \quad (i = 0, 1, 2\cdots N) \tag{5}$$

Here, $X(\tau_i)$ $(i = 0, 1, \cdots N)$ is discrete points of the state trajectory. Fig.3 shows the example of the discretized state trajectory. In the same way, the discrete points of the control trajectory $U(\tau_i)$ $(i = 1, 2, \cdots N)$ are defined using N nodes $\tau_i (i = 1, 2, \cdots N)$ and N Lagrange interpolating polynomials. In the following, we redefined the discrete points as $X_i \equiv X(\tau_i)$ and $U_i \equiv U(\tau_i)$.

The GPM is different from other Pseudospectral Methods in that the dynamics are not collocated at the boundary points. Therefore, terminal state $X_f \equiv X(\tau_{N+1})$ needs to be defined using $X_i (i = 0, 1, \cdots N)$. The equation defining the terminal state is given using the Gauss Quadrature as,

$$X_f \equiv X_0 + \frac{t_f - t_0}{2}\sum_{k=1}^{N} w_k f(X_k, U_k) \tag{6}$$

$$w_i = \frac{2}{(1-\tau_i^2)(\dot{P}_n(\tau_i))^2} \quad (i = 0, 1, 2\cdots N) \tag{7}$$

The Gauss Quadrature yields an exact result for polynomials of degree $2N-1$ or less.

3) The expression of the Dynamical System: The dynamical system $\dot{x} = f(x, u)$ is approximated using the variables X_i, U_i in the following equations.

$$\sum_{i=0}^{N} D_{ki} X_i - \frac{t_f - t_0}{2} f(X_k, U_k) = 0 \ (k = 1, 2, \cdots N) \tag{8}$$

Here, $D \in \mathbb{R}^{N\times N+1}$ is the differential approximation matrix. By applying the derivative of each Lagrange polynomial at the LG nodes, differential approximation matrix is given as follows.

$$D_{ki} = \dot{L}_i{}^{N+1}(\tau_k) = \sum_{l=0}^{N} \frac{\prod_{j=0, j\neq i,l}^{N}(\tau_k - \tau_j)}{\prod_{j=0, j\neq i}^{N}(\tau_i - \tau_j)} \tag{9}$$

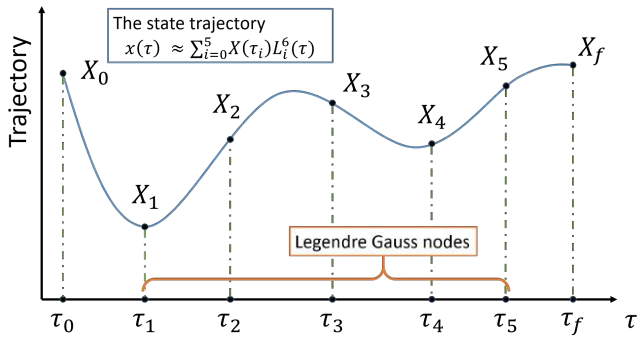

Fig. 3. Example: The state trajectory approximated by 6 th order Lagrange interpolation using 5 Legendre Gauss nodes.

B. Problem Formulation for COM Trajectory Optimization

1) One Step Motion Generation: In the biped locomotion, the contact constraints such as friction constraints may change at every step. For example, in the walking motion on the uneven terrain, the stability condition is changed according to the contact wrench cone of the uneven terrain. Therefore, it is better to regenerate the trajectory at every step using sensor feedback according to the environment. Besides, generating the trajectory with short cycle enables us to achieve faster convergence. From the above, we generate the COM trajectory at every step. Here, we predetermine step time and t_0 and t_f.

2) Dynamics: In our study, we calculate the COM trajectory considering centroidal dynamics. We assume zero variations of the angular momentum about the COM because it is difficult to control the angular momentum considering each limit of joint angles. The dynamics of COM is denoted by the sum of all external forces and moments in the following equations.

$$M\ddot{\boldsymbol{x}}_{COM} = \boldsymbol{F}_{all} - M\boldsymbol{g} \tag{10}$$

$$\mathbf{0} = (\boldsymbol{p}_{contact} - \boldsymbol{x}_{COM}) \times \boldsymbol{F}_{all} + \boldsymbol{\tau}_{all} \tag{11}$$

where M is the mass of the robot, $\boldsymbol{x}_{COM} = [x_{COM}, y_{COM}, z_{COM}]$ is the position of COM. F_{all}, τ_{all} is the sum of all external forces and moments. $\boldsymbol{p}_{contact}$ is the representative contact point.The representative contact point is the midpoint of the feet on the ground in the double support phase of walking motion. In the skating motion, the representative contact point is the foot which is fixed on the ground. Here, we define the frame whose origin is the representative contact point like Fig.4. From (10), (11), we discretize the COM position and velocity $\boldsymbol{x}_{COM}, \boldsymbol{v}_{COM}$

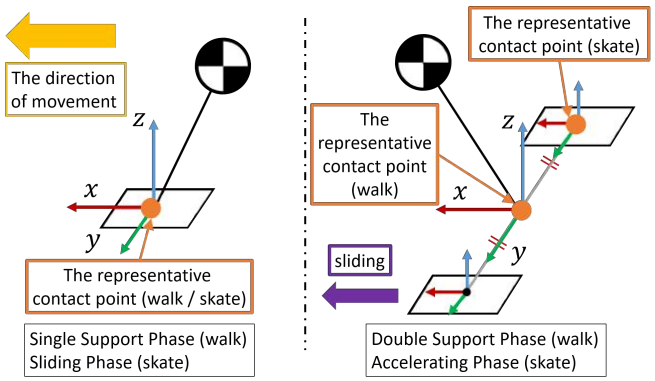

Fig. 4. The description of the frame and the representative contact point for the walking motion and skating motion.

and define the state variables as $X = [P_{COM}, V_{COM}] \in \mathbb{R}^{(N+2)\times 3}$. We also discretize the acceleration of the COM $\boldsymbol{a}_{COM}$ and define the control variables as $U = A_{COM} \in \mathbb{R}^{N\times 3}$. Furthermore, we introduce the simple dynamics $[\dot{\boldsymbol{x}}_{COM}, \dot{\boldsymbol{v}}_{COM}] = [\boldsymbol{v}_{COM}, \boldsymbol{a}_{COM}]$ and substitute these variables in (8) as follows.

$$\sum_{i=0}^{N} D_{ki} \left[P_{COM,i}, V_{COM,i}\right] - \frac{t_f - t_0}{2} \left[V_{COM,k}, A_{COM,k}\right] = \mathbf{0} \quad (k = 1, 2, \cdots N) \tag{12}$$

3) Cost Function: We define the cost function to minimize the acceleration of COM and described in the continuous-time as follows.

$$J = \frac{t_f - t_0}{2} \int_{-1}^{1} \left(\ddot{x}_{COM}(\tau)^2 + \ddot{y}_{COM}(\tau)^2 + \ddot{z}_{COM}(\tau)^2\right) d\tau \tag{13}$$

Thus, cost function is discretized using Gauss Quadrature from (7).

$$J = \frac{t_f - t_0}{2} \sum_{k=1}^{N} w_k A_{COM,k} A_{COM,k}^T \tag{14}$$

C. Constraints for Balancing and Large Acceleration

We describe three contact constraints and a kinematic constraint in this section. For the simplification, we apply contact constraints to the sum of all external forces and moments and consider the limitation of length between COM and the contact points for the kinematic constraints. Here, we discretize the normalized all external forces $\boldsymbol{F}_{all}/M$ and moments $\boldsymbol{\tau}_{all}/M$ to $F, N \in \mathbb{R}^{(N+1)\times 3}$. Using (10), (11), F, N is calculated by the state variables $X = [P_{COM}, V_{COM}]$ and the control variables $U = A_{COM}$ and the discretized representative contact point $P_0 \in \mathbb{R}^{N\times 3}$ in the following equations.

$$F_i = A_{COM,i} + \begin{bmatrix} 0 & 0 & g \end{bmatrix} \tag{15}$$

$$N_i = (P_{COM,i} - P_{0,i}) \times F_i \quad (i = 1, \cdots, N) \tag{16}$$

In the following, we formulate the constraints using the force F' and moment N' on the local coordinate system whose origin is the representative contact point.

1) Unilateral Constraints: We assume that the robot has unilateral ground contacts. Hence, the COM dynamics has a limitation imposed by the unilateral contact constraints as follows.

$$F'_{i2} \geq 0 \quad (i = 1, 2, \cdots, N) \tag{17}$$

2) Support Polygon Constraints: For simplification, we approximate co-planar contacts and impose the constraint that ZMP (Zero Moment Point) is within the support polygon made by its feet. We describe the support polygon constraints using M lines $a'_{ik}x + b'_{ik}y + c'_{ik} = 0 \ (k = 1, 2, \cdots, M)$ of each contact polygon's edge at each time i :

$$-a'_{ik}N'_{i1} + b'_{ik}N'_{i0} + c'_{ik}F'_{i2} \geq 0 \quad (i = 1, \cdots, N \quad k = 1, \cdots, M) \tag{18}$$

3) Friction Constraints: We consider friction constraints for large acceleration. The following inequality is given using static friction coefficient $\mu_{static,j} (j = 0, 1)$ for the static contact.

$$\|F'_{ij}\| \leq \mu_{static,j} F'_{i2} \quad (i = 1, \cdots, N \quad j = 1, 2) \tag{19}$$

In addition, we impose skating contact constraints for the linear sliding motion where dynamic friction coefficient is zero. We assume that all support legs are skating contacts in the linear sliding motion. Here, the equality is given using the sliding direction vector $d'_i \in \mathbb{R}^3$.

$$d'_i \circ F'_i = \mathbf{0} \tag{20}$$

4) Kinematic Constraints: We impose simple kinematic constraints to solve inverse kinematics as follows.

$$r_{min,i} \leq ||P_{COM,i} - P_{contact,i}|| \leq r_{max,i} \quad (i = 1, \cdots, N) \tag{21}$$

Here, r_{min}, r_{max} is minimum or maximum values of the distance between COM position and each contact points. $P_{contact,i}$ are contact points at at each time i.

D. Equality Constraints for Boundary Condition

We need to define boundary conditions to connect each trajectory for the one step motion generation. In our study, we give equality constraints for initial and final value.

1) Initial Condition: We set the initial condition that the initial state value is equal the final state value of one before trajectory for the continuity of motion in the following equality.

$$X_0^{current} = X_f^{before} \tag{22}$$

2) Terminal Condition using DCM and frictional constraints: When we stop the motion, we set the terminal condition as follows.

$$P_{COM,f} = P_{COM,f}^{ref} \tag{23}$$

$$V_{COM,f} = \mathbf{0} \tag{24}$$

where $P_{COM,f}, V_{COM,f}$ is the final state value.

Next, we set the terminal condition using DCM [1] and frictional constraints for connecting the trajectory at every step. First, the terminal condition for walk motion is described as follows by DCM Ξ_f.

$$\Xi_f = P_{COM,f} + bV_{COM,f} = P_{step} + \begin{bmatrix} 0 & 0 & \Delta z_{vrp}^{next} \end{bmatrix} \tag{25}$$

$$b = \sqrt{\Delta z_{vrp}^{next}/g} \tag{26}$$

where P_{step} is given reference foot step. Δz_{vrp} is the height difference between the contact point and the desired virtual repellent point (VRP) in the next trajectory and b is time constant. Next, in the skating motion, the next foot step has reference velocity. We assume sliding motion in the skating motion as the uniform linear motion. Therefore, the terminal condition is expanded by using the relative coordinate system which has the velocity in the following.

$$\begin{aligned} \Xi_f^{rel} &= P_{COM,f} + b\left(V_{COM,f} - V_{step}\right) \\ &= P_{step} + \begin{bmatrix} 0 & 0 & \Delta z_{vrp}^{next} \end{bmatrix} \end{aligned} \tag{27}$$

where V_{step} is the reference foot step velocity. In the walking motion, we define V_{step} as $\mathbf{0}$.

In addition, we need to evaluate the maximum acceleration for friction constraints for the connection to sliding phase in the skating motion. In our study, the acceleration of COM is approximated using LIP as follows in the continuous-time system.

$$\ddot{x} = \omega^2 \left(x - p_{step}\right) \tag{28}$$

where ω is $\omega = \sqrt{\frac{\ddot{z}+g}{z}}$. Here, when the next DCM corresponds with the reference ZMP, the COM monotonically converges to the reference ZMP. Therefore, the maximum acceleration of COM is the initial acceleration in the sliding phase. We add the following friction constraints in the direction of movement.

$$\|F_x\| = M\|\ddot{x}_{COM}\| \leq \mu_{static}^{next} F_z \tag{29}$$

Here we substitute (28) and $F_z = M(\ddot{z} + g)$ to (29)

$$||x_{COM} - p_{step}|| \leq \mu_{static}^{next} z_{COM} \tag{30}$$

Especially, the friction coefficient $\mu_{dynamic}^{next}$ is zero in the sliding phase of the skating motion. Hence the discretized friction constraint for the skating motion is in the following equation using the sliding direction vector $d_f \in \mathbb{R}^3$.

$$d_f \circ (P_{COM,f} - P_{step}) = \mathbf{0} \tag{31}$$

Additionally, we introduce the following equation to avoid a radical change of the acceleration at the transition from the accelerating phase to the sliding phase for the the real robot.

$$\sum_{k=1}^{N} \omega_k \sum_{i=0}^{N} D_{ki} d_f \circ U_i = 0 \tag{32}$$

where ω_k is the weight of Gauss Quadrature described as (7). and $D_{k,i}$ is the differential approximate matrix described as (9).

For the connection from the sliding phase to the accelerating phase, no terminal condition is imposed because the acceleration of COM is zero at all times in the sliding direction.

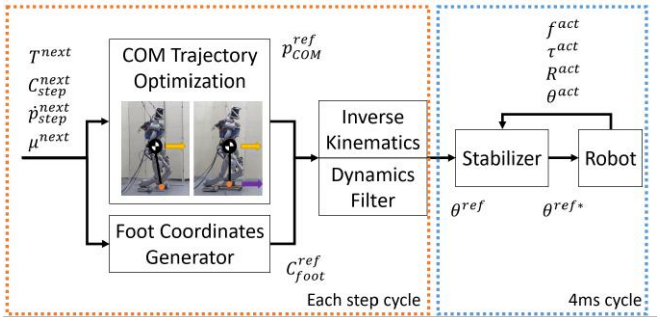

Fig. 5. Overview of proposed system

E. Nonlinear Optimization Problem

We transcribe the trajectory optimization to a nonlinear programming problem as follows.

$$\begin{aligned} \boldsymbol{Z}^* &= \arg\min_{\boldsymbol{Z}} J \\ C_{ineq}(\boldsymbol{Z}) &\geq \mathbf{0} \\ C_{eq}(\boldsymbol{Z}) &= \mathbf{0} \end{aligned} \tag{33}$$

where $\boldsymbol{Z} = \{X_0, X_f, X_i, U_i : i = 1, \cdots, N\}$ is optimization variables. C_{ineq} is inequality represented in (17), (18), (19), (21). C_{eq} is equality represented in (17), (18), (19), (21). We use scipy.optimize to solve this nonlinear programming problem by square least sequential quadratic programming (SLSQP) [23].

IV. Motion System for Real Robot

We describe the realization of the motion using COM trajectory generation explained in Section. III.

A. Overview of the Control

Fig.5 shows our proposed system using the nonlinear constrained COM trajectory optimization. First, we generate the COM trajectory at every step according to foot step parameters in the COM trajectory Optimization. The foot step parameters are double support time, single support time, next foot step position, next foot step velocity, and friction coefficient at the next foot step. Second, we generate the foot trajectory in the Foot Coordinates Generator. We provide the detail of Foot Coordinates Generator in Subsection. IV-B. Third, we solve the inverse kinematics [24] using the COM position and the foot coordinates. Next, we modify the reference trajectory to track reference ZMP using the Dynamics Filter of Kajita's Preview Controller [13]. Finally, the robot stabilizes by Kajita's Stabilizer [25] and executes the motion.

B. Foot Coordinates Generator

1) Walking Motion: We apply the cycloid for swing foot trajectory depend on the maximum height of the foot trajectory. The foot posture transit to the next foot posture by the linear interpolation.

2) Skating Motion: First, we generate the support foot trajectory by minimum jerk interpolation [26] according to the reference foot step position and velocity in the acceleration phase. In the sliding phase, we assume that the support foot performs the uniform linear motion. Next, we generate the swing foot trajectory using cycloid and minimum jerk interpolation.

C. Application to Walking and Skating motion

Table I shows the parameters we used for the discretization of the trajectory in the walking and skating motion. The data is collected on an Intel (R) Core (TM) i7-4790K CPU @ 4.00GHz. ACC is the accelerating phase and SLD is the sliding phase in the skating motion. As Table I shows, we found that the computation time of the COM trajectory generation is shorter than the motion duration.

TABLE I

THE PARAMETERS OF DISCRETIZATION

Parameter	Walk	Skate
node	10	10
motion duration	0.8 [s]	1.0 [s] (ACC) 2.0 [s] (SLD)
computation time	0.25 [s]	0.40 [s]

V. EXPERIMENTAL RESULTS

Experiments were conducted to evaluate the proposed method. We used a life-sized humanoid HRP-2 [27]. In the following experiments, we apply a world coordinate system.

A. Walking Motion

In this experiment, HRP-2 walked six steps with a stride length of 0.3 [m]. The span of single support phase is 0.6 [s] and the span of the double support phase is 0.2 [s].

Fig.6, Fig.7 shows the reference and actual trajectories of the COM and ZMP. As Fig.6, Fig.7 shows, the reference ZMP changed abruptly at the connection of each trajectory. The trajectory doesn't ensure the continuity of the acceleration because we use the minimum acceleration criterion for cost function. THe actual ZMP overshot due to the landing impact in Fig.7. We need to improve the reference foot trajectory and the feedback controller to reduce the landing impact.

Fig.8 shows the reference and actual height of the COM. We set the height of the reference DCM 0.80 [m]. The robot could change the height of COM according to the kinematics constraints not to stretch the limb.

Fig.9 shows the reference and actual velocity of the COM in the movement direction. The robot accelerated from 0 [m/s] to 0.40 [m/s] in 1.5 [s] and walked at 0.40 [m/s] and decelerated from 0.35 [m/s] to 0 [m/s] in 1.0 [s]. The robot could successfully change the velocity immediately.

B. Skating Motion

We demonstrated that HRP-2 executed fast skating motion on the skateboard to show the validity of our method. In this experiment, HRP-2 accelerated in 1.0 [s] and slid on the skateboard in 1.0 [s]. After sliding on the skateboard, HRP-2 stopped and transferred the initial state in 1.0 [s].

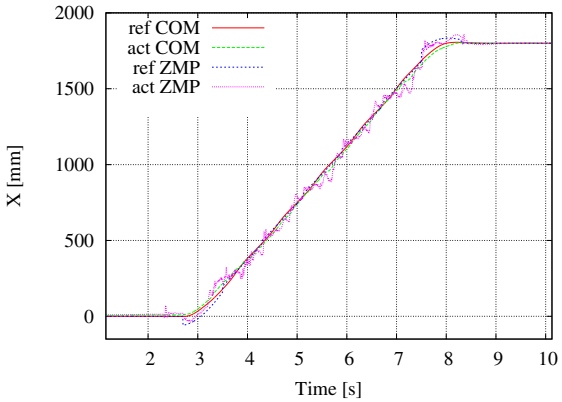

Fig. 6. The reference / actual position of COM and ZMP on the X axis in the walking motion

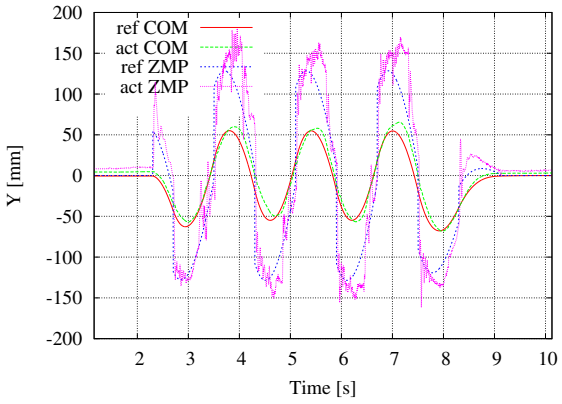

Fig. 7. The reference / actual position of COM and ZMP on the Y axis in the walking motion

Fig.10, Fig.11 shows the reference and actual COM and ZMP. We could not measure the actual ZMP in the world coordinate system because the skateboard and the force sensor moved in the direction of movement. Therefore, we plot the actual ZMP assuming that the actual ZMP is measured on the reference foot trajectory in the world coordinate system. In Fig.10, we could successfully control the COM and ZMP in the accelerating phase (4.1 [s] - 5.1 [s]). However, in the sliding phase (5.1[s] - 6.0 [s]), the actual ZMP swung around the reference ZMP. The balancing control using angular momentum is an issue in the future for more stable motion at the sliding phase. In Fig.11, we found that the actual ZMP didn't track the reference ZMP from 4.5 [s] to 5.1 [s]. The deviation is caused by our approximations. We need to consider the height of the skateboard and impose not only static contact constraints but also skating contact constraints in the accelerating phase.

Fig.12 shows the height of COM. The initial height of COM is 0.80 [m]. At the transition period between the accelerating phase and sliding phase, we set the height of the reference DCM 0.73 [m] and set the velocity of COM 0 [m/s] to prevent from reaching the limit of limb length.

Fig.13 shows the reference and the actual velocity of the root link in the direction of the movement. The actual velocity of the root link is measured by the IMU. The robot could successfully accelerate 0.0 [m/s] to 1.0 [m/s] in the

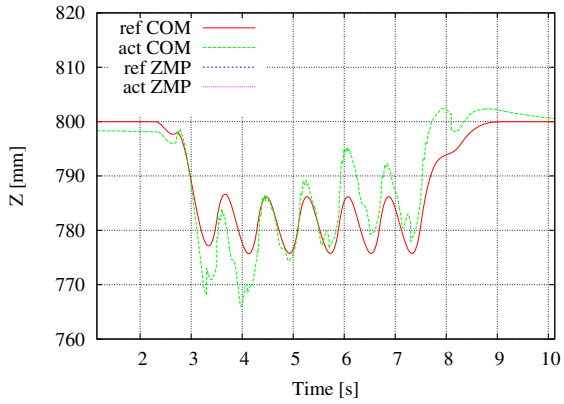

Fig. 8. The reference / actual position of COM on the Z axis in the walking motion

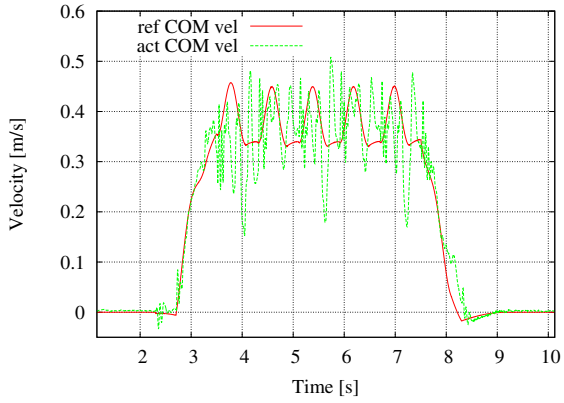

Fig. 9. The reference / actual velocity of COM on the X axis in the walking motion

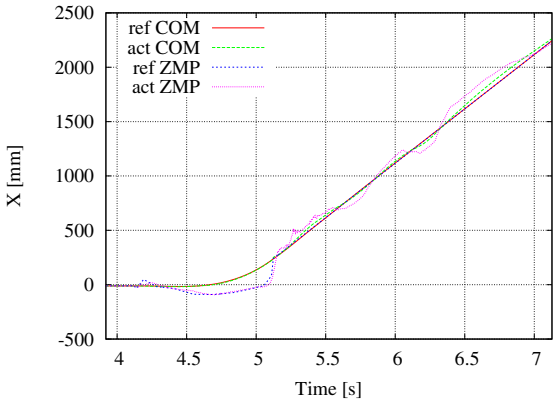

Fig. 10. The reference / actual position of COM and ZMP on the X axis in the skating motion

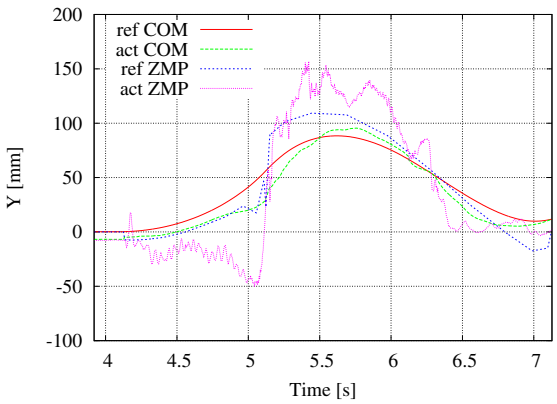

Fig. 11. The reference / actual position of COM and ZMP on the Y axis in the skating motion

accelerating phase (4.1 [s] - 5.1 [s]).

As Fig.14 shows, HRP-2 could skate on the skateboard with changing the height of COM without falling down.

VI. CONCLUSION

In this paper, we propose a 3D COM trajectory generation method for fast skating and walking motion. There are two important features about our methods. First, we introduce DCM and frictional constraints as the terminal condition to the connection of the trajectory optimization at every step. This enables us to generate not only walking but also skating motion. Second, by applying the Gauss Pseudospectral Method, we compute the fast 3D COM trajectory in less time than it requires to execute.

We evaluate the proposed method through the experiment using life-sized humanoid robot HRP-2. In the experiment, the robot could walk at 0.40 [m/s] using our method. We also showed the robot could accelerate from 0 [m/s] to 1.0 [m/s] in 1.0 [s] in the skating motion. In the accelerating phase of the skating motion, the actual zmp didn't track the reference zmp on the Y axis. We also found that the slight rotational slip occurred on the yaw axis in the walking and skating experiment. For solving these problems, it is necessary to take into account of contact constraints of each contact point instead of proposed approximated contact constraints of the total wrench. Therefore, it is a future task to generate more general motion which has multiple non-coplanar contacts considering force distribution in a short calculation time. In addition, we aim to regenerate the COM trajectory changing the foot placement using sensor feedback for robust and fast locomotion.

REFERENCES

[1] Johannes Englsberger, Christian Ott, and Alin Albu-Schäffer. Three-dimensional bipedal walking control based on divergent component of motion. *IEEE Transactions on Robotics*, Vol. 31, No. 2, pp. 355–368, 2015.

[2] Siyuan Feng, X Xinjilefu, Weiwei Huang, and Christopher G Atkeson. 3d walking based on online optimization. In *Proceedings of the 2013 IEEE-RAS International Conference on Humanoid Robots*, pp. 21–27. IEEE, 2013.

[3] C. Iverach-Brereton, A. Winton, and J. Baltes. Ice skating humanoid robot. In *Advances in Autonomous Robotics*, pp. 209–219. 2012.

[4] S. Jo, J. Chu, and Y. Lee. Motion planning for biped robot with quad roller skates. In *International Conference on Control, Automation and Systems, 2008*, pp. 1173–1177. IEEE, 2008.

[5] Noriaki Takasugi, Kunio Kojima, Shunichi Nozawa, Yohei Kakiuchi, Kei Okada, and Masayuki Inaba. Real-time skating motion control of humanoid robots for acceleration and balancing. In *Proceedings of the 2016 IEEE/RSJ International Conference on Intelligent Robots and Systems*, pp. 1356–1363. IEEE, 2016.

[6] S. Kajita, F. Kanehiro, K. Kaneko, K. Yokoi, and H. Hirukawa. The 3d linear inverted pendulum mode: A simple modeling for a biped walking pattern generation. In *Proceedings of The 2001 IEEE International Conference on Robotics and Automation*, pp. 239–246.

[7] K. Miura, S. Nakaoka, M. Morisawa, K. Harada, and S. Kajita. A friction based "twirl" for biped robots. In *Proceedings of the 2008 IEEE-RAS International Conference on Humanoid Robots*, pp. 279–284, Dec 2008.

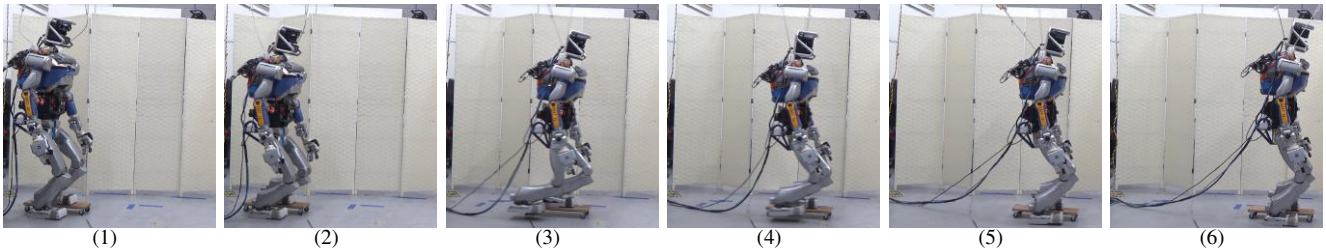

Fig. 14. HRP-2 accelerated and slid at 1.0 [m/s] in 1.0[s].

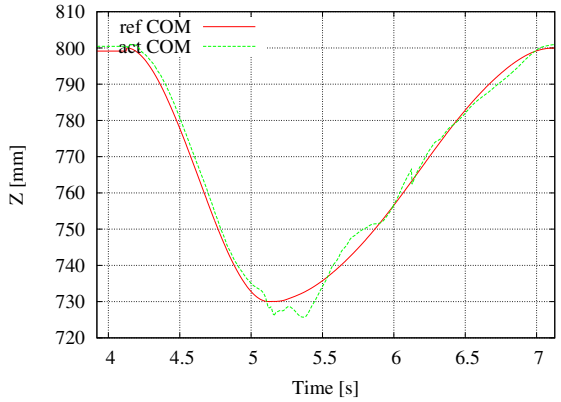

Fig. 12. The reference / actual position of COM and ZMP on the Z axis in the skating motion

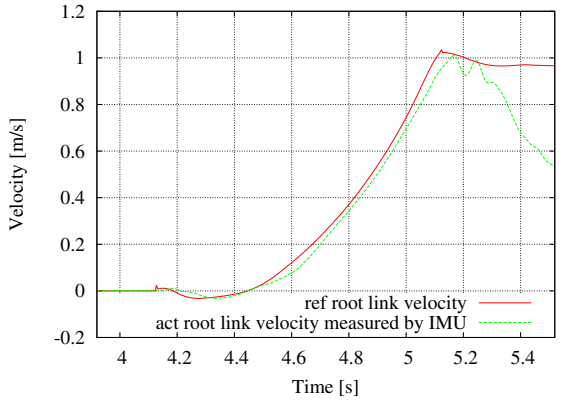

Fig. 13. The reference / actual velocity of the root link on the X axis measured by IMU

[8] K. Miura, S. Nakaoka, M. Morisawa, F. Kanehiro, K. Harada, and S. Kajita. Analysis on a friction based "twirl" for biped robots. In *Proceedings of The 2010 IEEE International Conference on Robotics and Automation*, pp. 4249–4255, May 2010.

[9] K. Miura, F. Kanehiro, K. Kaneko, S. Kajita, and K. Yokoi. Slip-turn for biped robots. *IEEE Transactions on Robotics,*, Vol. 29, No. 4, pp. 875–887, Aug 2013.

[10] K. Hashimoto, Y. Yoshimura, H. Kondo, Hun ok Lim, and A Takanishi. Realization of quick turn of biped humanoid robot by using slipping motion with both feet. In *Proceedings of The 2011 IEEE International Conference on Robotics and Automation*, pp. 2041–2046, May 2011.

[11] K. Kojima, S. Nozawa, K. Okada, and M. Inaba. Shuffle motion for humanoid robot by sole load distribution and foot force control. In *Proceedings of the 2015 IEEE/RSJ International Conference on Intelligent Robots and Systems*, pp. 2187–2194, Oct 2015.

[12] K. Hashimoto, Y Sugawara, T. Hosobata, Y. Mikuriya, H. Sunazuka, and M. Kawase. Sliding motion of biped walking robots mounted on passive wheels. *JSME Conference on Robotics and Mechatronics (In Japanese)*, pp. 11–11, 2007.

[13] S. Kajita, F. Kanehiro, K. Kaneko, K. Fujiwara, K. Harada, K. Yokoi, and H. Hirukawa. Biped walking pattern generation by using preview control of zero-moment point. In *Proceedings of The 2003 IEEE International Conference on Robotics and Automation*, pp. 1620–1626.

[14] S. Kajita, K. Kaneko, K. Harada, F. Kanehiro, K. Fujiwara, and H. Hirukawa. Biped walking on a low friction floor. In *Proceedings of the 2004 IEEE/RSJ International Conference on Intelligent Robots and Systems*, pp. 3546–3552.

[15] Russ Tedrake, Scott Kuindersma, Robin Deits, and Kanako Miura. A closed-form solution for real-time zmp gait generation and feedback stabilization. In *Proceedings of the 2015 IEEE-RAS International Conference on Humanoid Robots*, pp. 936–940.

[16] T. Takenaka, T. Matsumoto, T. Yoshiike, and S. Shirokura. Real time motion generation and control for biped robot-2 nd report: Running gait pattern generation. In *Proceedings of the 2009 IEEE/RSJ International Conference on Intelligent Robots and Systems*, pp. 1092–1099.

[17] Hongkai Dai and Russ Tedrake. Planning robust walking motion on uneven terrain via convex optimization. In *Proceedings of the 2016 IEEE-RAS International Conference on Humanoid Robots*, pp. 579–586. IEEE, 2016.

[18] Stéphane Caron, Quang-Cuong Pham, and Yoshihiko Nakamura. Zmp support areas for multicontact mobility under frictional constraints. *IEEE Transactions on Robotics*, 2016.

[19] M Kudruss, Maximilien Naveau, Olivier Stasse, Nicolas Mansard, C Kirches, Philippe Soueres, and K Mombaur. Optimal control for whole-body motion generation using center-of-mass dynamics for predefined multi-contact configurations. In *Proceedings of the 2015 IEEE-RAS International Conference on Humanoid Robots*, pp. 684–689. IEEE, 2015.

[20] Sébastien Lengagne, Joris Vaillant, Eiichi Yoshida, and Abderrahmane Kheddar. Generation of whole-body optimal dynamic multi-contact motions. *The International Journal of Robotics Research*, Vol. 32, No. 9-10, pp. 1104–1119, 2013.

[21] Ayonga Hereid, Shishir Kolathaya, and Aaron D Ames. Online optimal gait generation for bipedal walking robots using legendre pseudospectral optimization. In *2016 IEEE 55th Conference on Decision and Control (CDC)*, pp. 6173–6179. IEEE, 2016.

[22] David A Benson, Geoffrey T Huntington, Tom P Thorvaldsen, and Anil V Rao. Direct trajectory optimization and costate estimation via an orthogonal collocation method. *Journal of Guidance, Control, and Dynamics*, Vol. 29, No. 6, pp. 1435–1440, 2006.

[23] Jones E, Oliphant T, and Peterson P et al. Scipy: open source scientific tools for python. http://www.scipy.org/. 2001.

[24] Tomomichi Sugihara and Yoshihiko Nakamura. Whole-body cooperative balancing of humanoid robot using cog jacobian. In *Proceedings of the 2002 IEEE/RSJ International Conference on Intelligent Robots and Systems*, Vol. 3, pp. 2575–2580. IEEE, 2002.

[25] S. Kajita, M. Morisawa, K. Miura, S. Nakaoka, K. Harada, K. Kaneko, F. Kanehiro, and K. Yokoi. Biped walking stabilization based on linear inverted pendulum tracking. In *Proceedings of the 2010 IEEE/RSJ International Conference on Intelligent Robots and Systems*, pp. 4489–4496.

[26] Bruce Hoff and Michael A Arbib. Models of trajectory formation and temporal interaction of reach and grasp. *Journal of motor behavior*, Vol. 25, No. 3, pp. 175–192, 1993.

[27] K. Okada, T. Ogura, A. Haneda, J. Fujimoto, Fabien Gravot, and M. Inaba. Humanoid motion generation system on hrp2-jsk for daily life environment. In *IEEE International Conference Mechatronics and Automation, 2005*.